Catalysis Today 174 (2011) 70–78

Contents lists available at ScienceDirect

Catalysis Today

journal homepage: www.elsevier.com/locate/cattod

Aerosol processing of mesoporous silica supported bimetallic catalysts for low temperature acetone oxidation

Chen Yeh Wang, Hsunling Bai*

Institute of Environmental Engineering, National Chiao Tung University, 1001 University Road, Hsinchu 300, Taiwan

ARTICLE INFO

Article history:
Received 26 October 2010
Received in revised form 10 February 2011
Accepted 16 February 2011
Available online 22 March 2011

Keywords:
VOCs
Mesoporous silica materials
Acetone oxidation
Evaporation induced self assembly method
Cerium oxide catalyst
Aerosol spray

ABSTRACT

One step aerosol EISA (evaporation induced self-assembly) process for synthesizing Ce/metal–MSPs (mesoporous silica spherical particles) catalysts was investigated. The catalysts were then applied to the catalytic oxidation of acetone. The TEM images showed that increasing Ce/Al loading resulted in clearer observation of the metal oxide particles on the MSPs surface, but an excessive metal quantity would destroy the mesoporous structure of the MSPs support. Tests on the monometallic Ce–MSPs and bimetallic Ce/Al–, Ce/Mn- and Ce/Cu–MSPs under temperatures of 150–350 °C demonstrated that Ce/Al–MSPs had the best acetone removal at low temperature ranges of less than 200 °C, and it could have ~80% acetone removal at reaction temperature of 150 °C, space velocity of 15,000 h^{-1} and acetone inlet concentration of 1000 ppmv. The synergetic effect was observed for bimetallic Ce/Al–MSPs on the acetone removal as compared to the monometallic Ce–MSPs or Al–MSPs catalysts. The Al loading amount, BET specific surface area and the CeO_2 particle size played important roles on the low temperature catalytic oxidation of acetone at 150 °C. The acetone removal of both Ce–MSPs(25) (the molar ratio of Si/Ce = 25) and Ce/Al–MSPs(50/50) (the molar ratio of Si/Ce = 50 and Si/Al = 50) exhibited good stability at 250 °C but decayed gradually at 150 °C after 24 h tests.

1. Introduction

Catalytic oxidation has been known as one of the most promising techniques for VOCs abatement due to its lower operation temperature (<500 °C) which reduces energy cost and results in less amounts of toxic products as well [1]. Cerium oxide (CeO_2) catalysts used alone or mixed with other metal oxides have been attracted much attention for the VOCs removal because cerium is the most abundant of the Lanthanide-based metals and CeO_2 has high oxygen-storage capacity and facile Ce^{4+}/Ce^{3+} redox cycle [2,3]. Recent reports have shown that the performance of CeO_2 which can efficiently eliminate trichloroethylene [4], naphthalene [5], and toluene [6]. There are also reports on the performance of bimetallic Ce-based catalysts, e.g. Ce/Mn oxides for the oxidation of o-xylene [7], Ce/Cu oxides for acetone, ethanol, ethyl acetate, and toluene oxidation [8,9] as well as Ce/Al oxides for toluene oxidation [10]. The CeO_2 was also used as a support for low temperature oxidation of ethyl acetate over precious metal catalysts [11].

There are several studies investigated on the VOCs abatement at low reaction temperature. The noble metal of Pt was supported on either styrene divinylbenzene copolymer or MCM-41 for the destruction of toluene at 150 °C [12,13]. Aube [14] prepared perovskite-type $La_{0.8}Sr_{0.2}MnO_{3+x}$ catalyst by using citric acid sol–gel method and obtained about 75% acetone oxidizing performance at the reaction temperature of 150 °C. More recently, silica-based mesoporous materials have been widely explored as supports due to their high surface area and uniform pore size distribution. Metal catalysts supported on the mesoporous silica materials of Ce–MCM-41[15], Cu/Mn–MCM-41[16] and Co/Ce–SBA-15[17] were prepared for the VOCs abatement. The hydrophobicity, activity, and pore characteristics of the catalyst support are very important for catalytic combustion [18]. And it was demonstrated that MCM-41, when surface-modified with fluoride anions, is better than ZSM-5 as a catalyst support due to its high hydrophobicity and uniform pore structure [13].

The mesoporous silica spherical particles (MSPs) were synthesized via an aerosol evaporation induced self-assembly (EISA) method as an intention on simplifying the preparation procedure of MCM-41 [19]. The MSPs ensure fast and simple production of mesoporous materials as compared to the manufacturing of MCM-41 materials. In addition, it has been demonstrated that the volume-based acetone adsorption capacity is higher than that of MCM-41, and the pressure drop of MSPs in an adsorber is lower than that of MCM-41 [20,21].

To the authors' knowledge, there are limited reports on preparing metal-MSPs by one step aerosol EISA method. The MSPs

* Corresponding author. Tel.: +886 3 5731868, fax: +886 3 5725958.
E-mail address: hlbai@mail.nctu.edu.tw (H. Bai).

0920-5861/$ – see front matter © 2011 Elsevier B.V. All rights reserved.
doi:10.1016/j.cattod.2011.02.025

containing Al or Zr were synthesized via the aerosol EISA method [22] and the results showed that the incorporation of these metals was more hydrothermally stable than pure mesoporous silica. The noble metal incorporated MSPs were synthesized and tested as a catalyst in the hydro-dechlorination reaction of 1,2-dichloroethane and it exhibited near complete conversion and ethylene selectivity at 350 °C [23]. Noble metals of Au were deposited on the MSPs via the amine functionalization method [24]. And the catalyst of Au–NH_2–Co–MSPs showed the highest reactivity for CO oxidation, suggesting that the nature of the support is very important for this reaction.

Our prior research results [25] indicated that among tested monometallic catalysts of Ce, Mn, Cu, Fe and Al–MSPs, the Ce–MSPs appear to have the best performance on acetone oxidation. This study intends to present on the performance of cerium-based bimetallic MSPs for the oxidation of acetone vapors. The bimetallic (Ce/Al, Ce/Mn and Ce/Cu) catalysts supported on the MSPs are tested, and those which have higher acetone removals at relatively lower temperatures are chosen for further detailed study.

2. Materials and methods

2.1. Synthesis of catalytic mesoporous materials

Three metals, Mn, Cu, and Al, were chosen as the metal species to mix with Ce for synthesizing the bimetallic Ce/metal–MSPs catalysts. The metal precursors were prepared from cerium nitrate, manganese nitrate, copper nitrate, and aluminum nitrate solutions, respectively. Cetryltrimethylammonium bromide (CTAB) was used as the structure directing template and tetraethoxysilane (TEOS) was used as the silicon precursor for obtaining the mesoporous structure of silica supports. The molar gel composition of the synthesized mixture was 1 SiO_2: 0.18 CTAB: 10 ethanol: 80 H_2O: 0.008 HCl: 1/X metal. The synthesized samples are denoted as Ce/metal–MSPs (X_1/X_2), where X_1 corresponded to the molar ratio of Si/Ce and X_2 corresponded to the molar ratio of Si/metal in the precursor solution.

All of the precursors were mixed together and stirred for 30 min to obtain a clear solution. The solution was then nebulized by an ultrasonic atomizer (1.8 MHz) and the atomized droplets were passed through two heaters by a dry and clean air stream with flow rate maintained at 2LSTP min^{-1}. The first and second heating zones of the aerosol process were controlled at temperatures of 150 and 550 °C, respectively. After the evaporation of the surfactant and solvents, metal catalysts supported on mesoporous silica particles were obtained and collected on a filter. They were then further calcined at 550 °C for 6 h in air. Detailed procedures on the EISA aerosol method can be referred to our prior study [20].

2.2. Characterization of catalysts

The specific surface area, specific pore volume and average pore diameter (BJH method) of the samples were measured by N_2 adsorption–desorption isotherm at 77 K using a surface area analyzer (Micromeritics, ASAP 2020, USA). Prior to the adsorption–desorption measurements, the samples were degassed at 350 °C for 6 h under vacuum pressure of 10^{-6} mbar. The elemental metal contents in the catalysts were analyzed by an inductively coupled plasma-mass spectrometer (ICP-MS, SCIEX ELAN 5000). X-ray Diffraction (XRD) patterns of calcined samples were recorded by a Rigaku X-ray diffractometer equipped with nickel-filtered CuKα (λ = 1.5405 Å) radiation. The diffraction diagrams of the mesoporous samples were recorded in the 2θ range of low-angles at 2–10° and wide-angles at 10–80°. Transmission electron microscopy (TEM) images of the samples were observed with a JEOL JEM 1210 instrument, before that the samples were ultrasonicated in ethanol and dispersed on carbon film supported on copper grids (200 mesh).

2.3. Catalytic oxidation of acetone

The acetone is chosen as the target volatile organic compound, which is commonly used as a solvent in chemical and semiconductor processing plants. The oxidation of acetone was carried out by a vertical and downward flow catalytic reactor system. The reactor was made of Pyrex glass tube with 0.8 cm internal diameter. The reactor was heated to the desired temperature with a tubular furnace. Catalysts were tested in 16–30 mesh powdered form and placed in the middle of the glass reactor supported with thin layers of glass wool on both sides. The concentration of acetone was controlled by passing the clean and compressed air through an impinger containing liquid acetone that was kept in a constant temperature-controlled water bath at −10 °C. The total inlet flow rate was controlled to have a GHSV of 15,000 h^{-1} at room temperature (25 °C). The inlet and outlet concentrations of acetone were

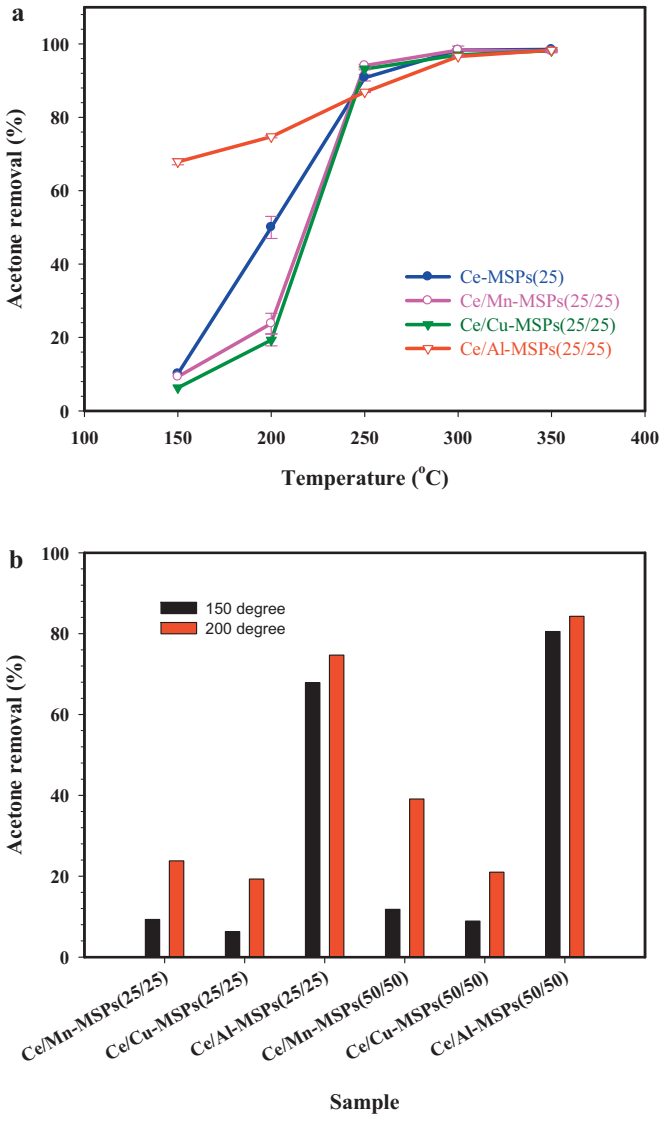

Fig. 1. (a) Acetone removals of monometallic Ce–MSPs(25) and bimetallic Ce/metal–MSPs(25/25) (metal = Mn, Cu, Al) catalysts. (b) Comparison of acetone removals for bimetallic Ce/metal–MSPs(25/25) and (50/50) (metal = Mn, Cu, Al) catalysts at low temperatures.

Table 1
Physical and chemical properties of metal–MSPs.

Sample name	Si/Ce[a] molar ratio	Si/Al[a] molar ratio	Si (wt.%)	Ce (wt.%)	Al (wt.%)	Si/Ce[b] molar ratio	Si/Al[b] molar ratio	Vp[c] (cm^3/g)	S_{BET}[d] (m^2/g)	d_{BJH}[e] (nm)
Ce–MSPs(10)	10	0	23.0	9.8	0	11.8	0	0.49	615	2.81
Ce–MSPs(25)	25	0	25.3	3.7	0	34.0	0	0.73	951	2.56
Ce–MSPs(50)	50	0	28.7	1.9	0	76.4	0	0.80	1003	2.54
Al–MSPs(10)	0	10	–	–	–	–	–	0.57	787	2.70
Al–MSPs(50)	0	50	–	–	–	–	–	0.83	1053	2.54
Al–MSPs(200)	0	200	–	–	–	–	–	0.88	1098	2.53
Ce/Al–MSPs(10/10)	10	10	25.4	12.5	2.7	10.2	8.9	0.33	228	4.56
Ce/Al–MSPs(10/50)	10	50	–	–	–	–	–	0.24	309	2.89
Ce/Al–MSPs(10/200)	10	200	–	–	–	–	–	0.34	414	2.91
Ce/Al–MSPs(25/10)	25	10	–	–	–	–	–	0.47	578	2.64
Ce/Al–MSPs(25/25)	25	25	32.1	5.9	1.1	27.1	29.1	0.62	785	2.66
Ce/Al–MSPs(25/50)	25	50	–	–	–	–	–	0.59	793	2.65
Ce/Al–MSPs(25/200)	25	200	–	–	–	–	–	0.44	853	2.44
Ce/Al–MSPs(50/10)	50	10	–	–	–	–	–	0.49	677	2.63
Ce/Al–MSPs(50/25)	50	25	33.1	2.7	1.2	60.4	27.0	0.71	917	2.53
Ce/Al–MSPs(50/50)	50	50	33.8	2.7	0.7	61.9	45.1	0.75	971	2.49
Ce/Al–MSPs(50/200)	50	200	25.8	2.8	0.1	46.2	205.7	0.76	979	2.52
Ce/Mn–MSPs(25/25)	25	25(Si/Mn)	–	–	–	–	–	0.49	415	3.91
Ce/Cu–MSPs(25/25)	25	25(Si/Cu)	–	–	–	–	–	0.52	538	3.42
Ce/Mn–MSPs(50/50)	50	50(Si/Mn)	30.9	2.7	1.3_{Mn}	57.8	47.2Si/Mn	0.73	893	2.64
Ce/Cu–MSPs(50/50)	50	50(Si/Cu)	29.1	3.5	1.0_{Cu}	42.1	67.4Si/Cu	0.73	930	2.60
MSPs	0	0	–	–	–	–	–	0.90	1153	2.40

[a] Si/Ce and Si/Al molar ratio calculated based on the precursor concentration.
[b] Actual Si/Ce and Si/Al molar ratio measured by ICP-MS.
[c] Pore volume.
[d] BET surface area.
[e] Pore diameter calculated by BJH theory.

analyzed by a gas chromatograph (GC 7890A, Agilent) equipped with a flame ionization detector (FID). The removal efficiency of acetone was defined by that

$$\text{Removal}\,(\%) = \frac{I - O}{I} \times 100\%,$$

where I and O are the inlet and outlet concentrations of acetone, respectively.

3. Results and discussion

3.1. Comparing the Acetone removals of Ce/metal–MSPs

Except stated otherwise, results of all catalytic incineration tests were shown under the base condition of 1000 ppmv acetone concentration, 15,000 h^{-1} space velocity, and 30 min operation time. The acetone catalytic performance of bimetallic Ce/metal–MSPs(25/25) (metal = Mn, Cu, Al) and monometallic Ce–MSPs(25) is depicted in Fig. 1(a) as a function of temperature with error bars indicate the range of three repeated tests. It was observed that all of the samples had similar acetone removal efficiencies at temperatures above 300 °C. The acetone removals of Ce/Mn–MSP(25/25), Ce/Cu–MSP(25/25) and Ce–MSPs(25) were slightly higher than that of Ce/Al–MSPs(25/25) at 250 °C. But at low temperatures of 150–200 °C, the Ce/Al–MSPs(25/25) had much higher acetone removals than all other catalysts. Fig. 1(b) showed the acetone oxidation at temperature of 150 °C and 200 °C for Ce/Mn-, Ce/Cu-, Ce/Al–MSPs(25/25) and (50/50). At the low temperature of 150 °C, the presence of Al in the Ce/Al–MSPs(25/25) and Ce/Al–MSPs(50/50) enhanced the acetone removal to 68% and 80.5% respectively, while the Ce mono-metal or Ce/Mn and Ce/Cu bimetals supported on the MSPs had only less than 10 and 40% acetone removals, respectively, at 150 and 200 °C.

The specific surface area of Ce/Al–MSPs(25/25) and Ce–MSPs(25) were 785 and 951 m^2/g, respectively. They were much higher than that of Ce/Cu–MSPs(25/25), 538 m^2/g, and Ce/Mn–MSPs(25/25), 415 m^2/g. Because Al has a similar atomic size to Si, it could partially replace Si into the Si–O–Si chemical bonds of the mesoporous silica support without significantly destroy the pore structure. Thus although Mn and Cu could have high activity at high reaction temperature (>250 °C), the low surface area of their supports could possibly inhibit their activity at low temperatures where adsorption might play an important role. On the other hand, the specific surface area of Ce/Al–MSPs(50/50) and Ce–MSPs(50) were 971 and 1003 m^2/g, respectively. They were slightly higher than those of Ce/Cu–MSPs(50/50), 930 m^2/g, and Ce/Mn–MSPs(50/50), 893 m^2/g. This indicates the less damage in the pore structure of the Ce/metal–MSPs(50/50) as compared to the Ce/metal–MSPs(25/25). However as observed in Fig. 1(b), the acetone removals via Ce/metal–MSPs(50/50) with less metal contents were still higher than that of Ce/metal–MSPs(25/25) due to their higher surface area and smaller CeO_2 particle size.

Since Ce/Al–MSPs appears to be the best bimetallic combination for the oxidation of acetone at relatively low temperature range of 150–200 °C, the following study is focused on the Ce/Al–MSPs for their effectiveness on acetone removal.

3.2. Characterization of the Ce/Al–MSPs catalysts

The chemical and physical properties of metal–MSPs are listed in Table 1. For the Ce–MSPs with Si/Ce precursor molar ratio from 50 to 10, the actual Ce contents ranged from 1.9 to 9.8 wt.% as characterized by ICP-MS. And for the bimetallic Ce/Al–MSPs(50/50), (25/25), and (10/10) with Si/Ce and Si/Al precursor molar ratios from 50 to 10, the actual Ce contents ranged from 2.7 to 12.5 wt.% while Al contents ranged from 0.7 to 2.7 wt.%. When increasing the loading amount of either Al or Ce metal, the specific surface area of the catalysts was decreased due to the destruction of silica pores during the one step aerosol EISA synthesis process. The Ce/Al–MSPs(10/10) had the lowest specific surface area of only 228 m^2/g. From the results of the pore size, it indicated that all samples were in the range of mesoporous structure (2 nm < d < 50 nm). And all samples had average pore diameters of less than 3 nm except the Ce/Al–MSPs(10/10) which BJH pore diameter was 4.56 nm.

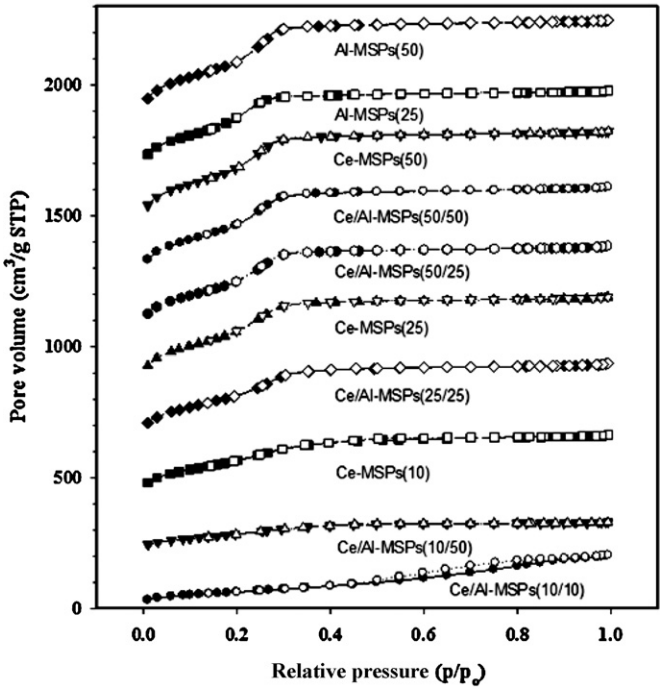

Fig. 2. Nitrogen adsorption–desorption isotherms (adsorption: closed symbols; desorption: opened symbols) of Ce–MSPs, Al–MSPs, and Ce/Al–MSPs catalysts. In the y-axis, values of each catalyst were stepwise increased by 200 cm^3/g starting from the bottom catalyst (Ce/Al–MSPs(10/10)).

The nitrogen adsorption–desorption isotherms of bimetallic Ce/Al–MSPs catalysts are depicted in Fig. 2. All the tested samples appeared to have the type IV isotherms based on IUPAC classification and exhibited mesoporous structure. But the type IV isotherm shapes of Ce/Al–MSPs(10/10) and Ce/Al–MSPs(10/50) were not as clear as the other catalysts. Besides, for most of the tested catalysts except the Ce/Al–MSPs(10/10), the sharp increases in the quantity of nitrogen adsorption were observed at relative pressures (p/p_0) of around 0.3. As observed from Table 1, the Ce/Al–MSPs(10/10) had the lowest BET surface area and the largest BJH pore size of all tested catalysts, while the Ce/Al–MSPs(10/50) had the lowest pore volume of all samples. So the mesoporous structure of these two catalysts was poorer than that of the other catalysts.

Fig. 3(a) shows the BJH pore size distributions of Ce–MSPs(50) and Ce/Al–MSPs(50/X_2), Fig. 3(b) show the BJH pore size distributions of Ce–MSPs(25) and Ce/Al–MSPs(25/X_2), and Fig. 3(c) show the BJH pore size distributions of Ce–MSPs(10) and Ce/Al–MSPs(10/X_2) catalysts, respectively. When the MSPs contained less Ce, as seen in Fig. 3(a), the pore volume at peak pore diameter was larger and the pore size distribution was more uniformly distributed than more Ce presented in the MSPs as seen in Fig. 3(b) and (c). And if more Ce was presented on the MSPs support, an additional peak in the pore size distribution appeared at >30 Å as observed in Fig. 3(c). The second peaks of all samples observed in Fig. 3(c) might reveal partial collapse of the ordered pores or the formation of agglomerated metal oxide particles which resulted in inter-particle pores. But as also seen in Fig. 3(c),

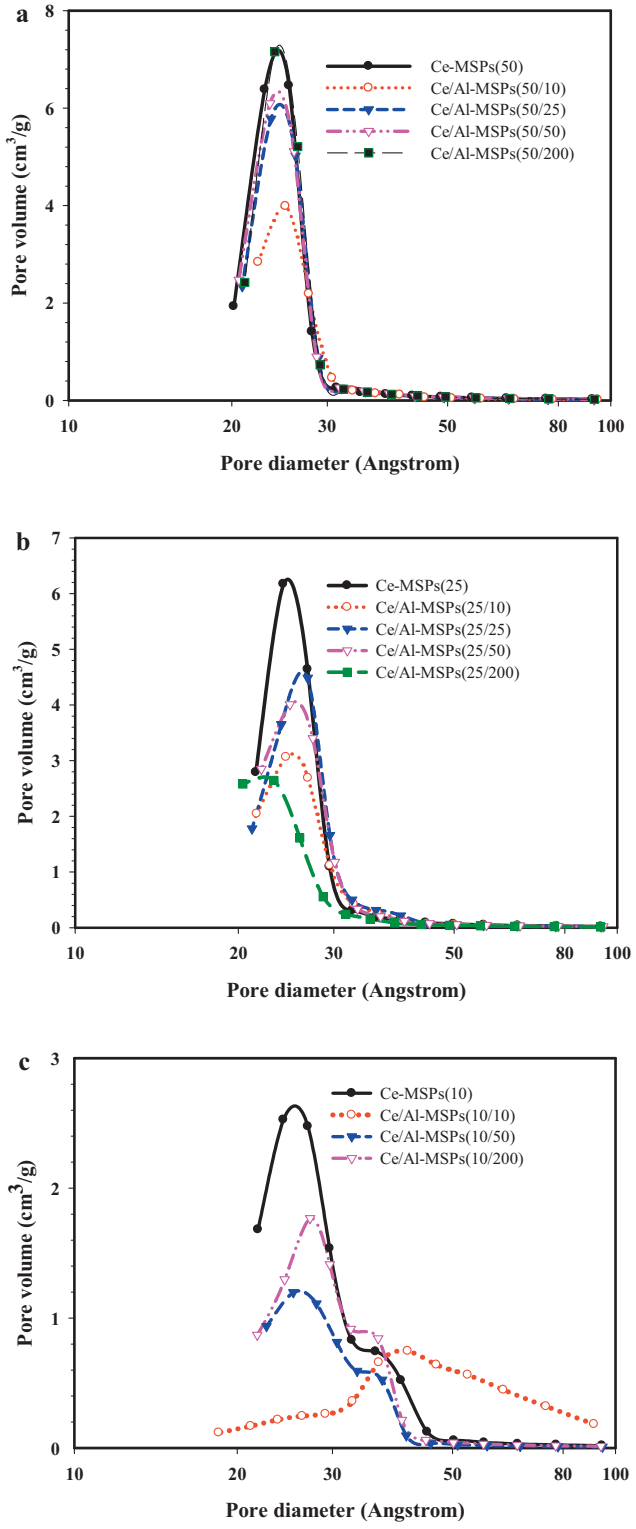

Fig. 3. (a) BJH pore size distributions of Ce–MSPs(50) and Ce/Al–MSPs(50/X) catalysts. (b) BJH pore size distributions of Ce–MSPs(25) and Ce/Al–MSPs(25/X) catalysts. (c) BJH pore size distributions of Ce–MSPs(10) and Ce/Al–MSPs(10/X) catalysts.

Ce–MSPs(10), Ce/Al–MSPs(10/200) and Ce/Al–MSPs(10/50) have primary pore size distribution peaks and shoulder peaks as well, whereas Ce/Al–MSPs(10/10) has only a broad pore size distribution peak with a larger average pore size. Therefore it also appears that as the Al loading was increased the mesoporous structure of Ce/Al–MSPs(10/X_2) became more disordered.

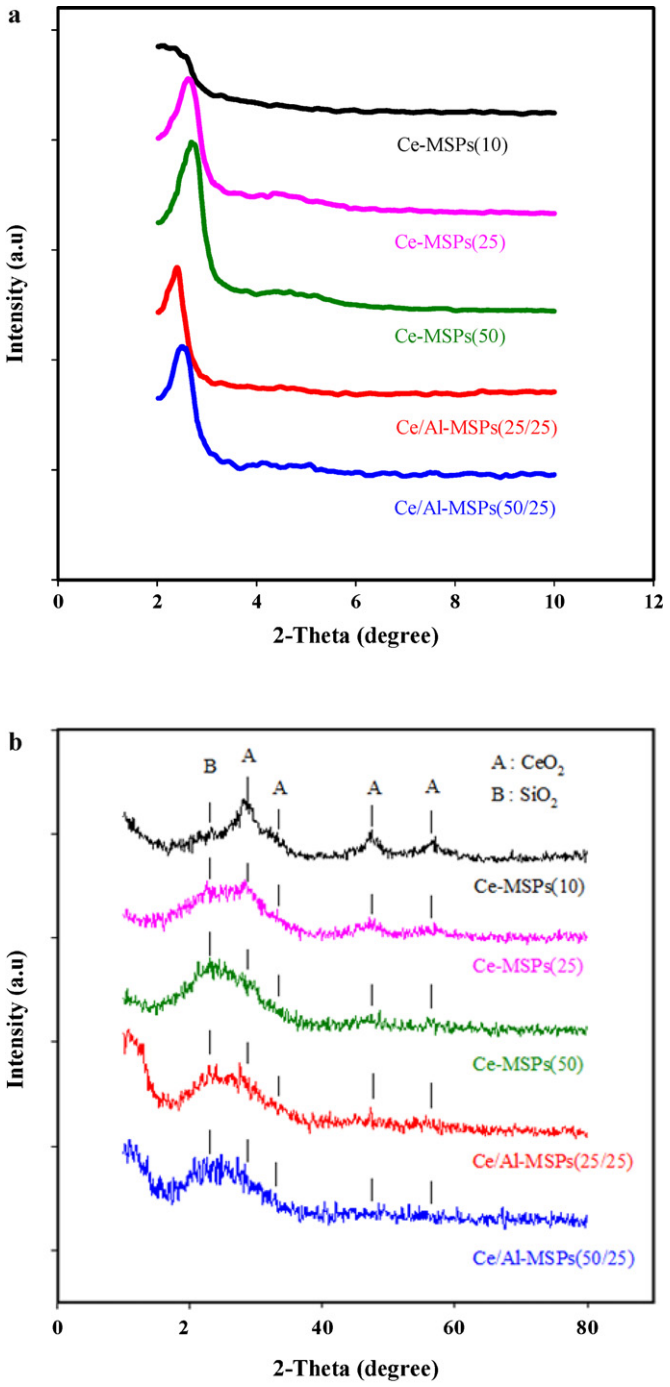

Fig. 4. (a) Low angle X-ray diffraction patterns of Ce–MSPs and Ce/Al–MSPs catalysts. (b) Wide angle X-ray diffraction patterns of Ce–MSPs and Ce/Al–MSPs catalysts.

The low angle ($2 \leqq 2\theta \leqq 10^\circ$) and wide angle ($10 \leqq 2\theta \leqq 80^\circ$) XRD patterns of Ce/Al–MSPs are depicted in Fig. 4(a) and (b), respectively. The (1 0 0) diffraction peaks located at about $2\theta = 2.3$–2.7° were observed from the low angle XRD patterns of Fig. 4(a) for all samples except for Ce–MSPs(10). This revealed the evidence of mesoporous structure [20,26]. As seen in Fig. 2, the Type IV Isotherm curve was also not well-defined for Ce–MSPs(10). This suggests a partial collapse of the mesoporous structure for Ce–MSPs(10), which agreed with its low-angle XRD pattern in Fig. 4(a). The shape of the XRD peak shifted to the left as the Ce or Al contents were increased. From the wide angle XRD patterns shown in Fig. 4(b), the 2θ peak at about 23° was due to the

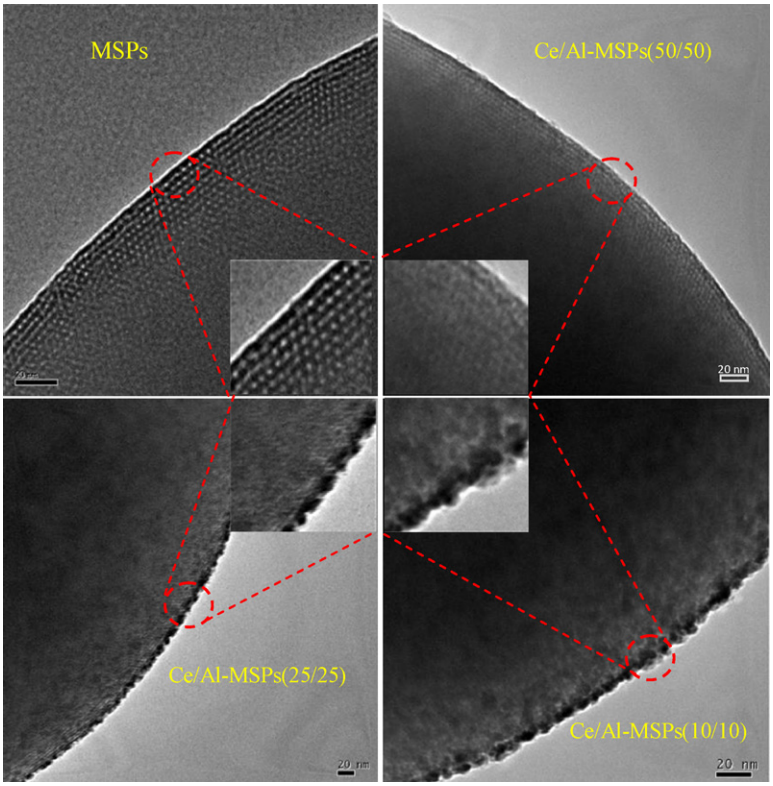

Fig. 5. TEM images of MSPs and Ce/Al–MSPs: MSP, Ce/Al–MSPs(50/50), Ce/Al–MSPs(25/25), Ce/Al–MSPs(10/10); all images has the same scale bar of 20 nm. And the images located in the center were partially enlarged to provide clearer observations of the metal particles and the pore structure.

amorphous silica [23]. And increasing the Ce content in the Ce/Al–MSPs sample resulted in stronger CeO2 intensity at $2\theta = 28.8$, 33.3, 47.5 and 56.4° [4,17] as observed most clearly for the Ce–MSPs(10) catalyst. The clear observation of CeO_2 peaks revealed that the CeO_2 particles on the MSPs support might be presented in larger particle sizes or in agglomerated form. This further confirmed the data shown in Table 1 and Fig. 3(c) that when loaded with more metal amount, not only the specific surface area would be reduced but also the metal oxide particles might be larger.

The TEM images of pure MSPs and Ce/Al–MSPs are shown in Fig. 5. One can see that for the pure MSPs without loading any metals, the hexagonal pores were clearly seen with highly ordered arrangement. Increasing Ce/Al loading resulted in a more clear observation of the metal oxides particles on the surfaces of the MSPs. But the pore structure became less clear as the Ce/Al metal content was increased. The partial collapses of the pore structure due to increasing metal content and the clearer observation of the metal oxide particles were in accord with the BET measurement data and the XRD patterns. Nevertheless the TEM images show that the CeO_2 particles still appeared to be well dispersed on the surfaces of all Ce/Al–MSPs as compared to the metal–MCM-41 catalysts manufactured via the two-step hydrothermal and ion-exchanged method [16]. This indicated that the one-step aerosol EISA method could produce well dispersed metal oxides on the porous silica supports.

3.3. Metal loading vs. BET surface area

Ce/Al–MSPs catalysts of three different Ce loading amounts (Si/Ce = 10, 25 and 50) were prepared together with four different loading amounts of Al (Si/Al = 10, 50, 200 and 0) to study the simultaneous metal loading and surface area effects on the acetone removal. The results are shown in Fig. 6 for reaction temperatures of

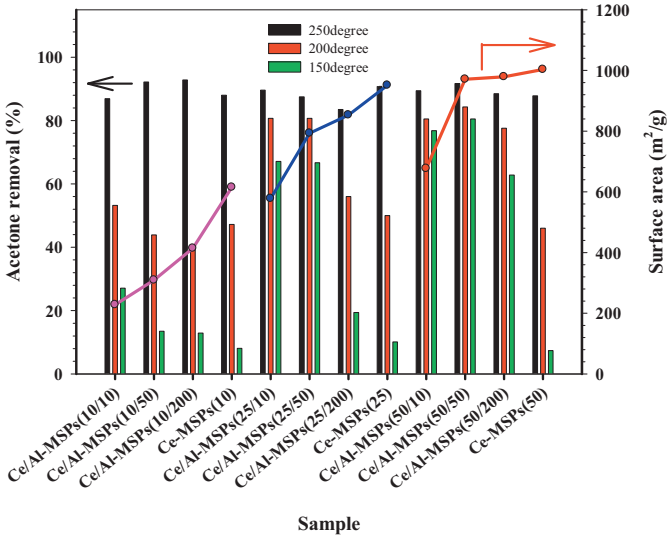

Fig. 6. The correlation between acetone removal, specific surface area for Ce–MSPs and Ce/Al–MSPs at temperature of 150, 200, and 250 °C.

150, 200 and 250 °C. It was observed that at relatively higher temperature of 250 °C, both BET surface area and metal loading amount had negligible effects on the acetone removal. But at low temperature of 150 °C the surface area and the metal loading effects became very significant.

For the same Ce loading, reducing the Al content resulted in higher BET surface area but lower acetone removal at 150 °C. But for the same loading of Al, reducing the Ce content led to both higher BET surface area and higher acetone removal. And among all samples which have high surface areas of around 1,000 m^2/g, as seen for the Ce–MSPs(25), Ce/Al–MSPs(50/50), Ce/Al–MSPs(50/200) and

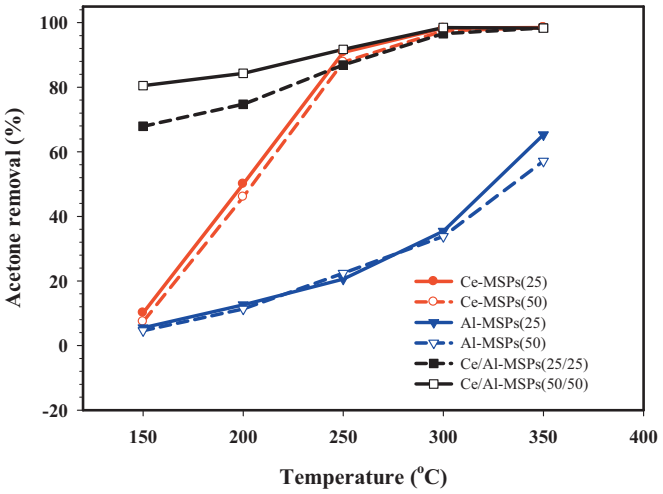

Fig. 7. Effect of temperature on the acetone removal via Ce–MSPs, Al–MSPs, and Ce/Al–MSPs.

Ce–MSPs(50) catalysts, the Ce/Al–MSPs(50/50) with the highest Al content appeared to have the highest acetone removal at low temperature of 150 °C. But even though Ce/Al–MSPs(50/10) has a lower surface area, the efficiency of its acetone removal is almost as good as that for Ce/Al–MSPs(50/50). This revealed that the Al loading amount, CeO_2 particle size and the BET specific surface area played important roles on the low temperature catalytic oxidation of acetone. It appeared that the amount of metals loading was correlated with the CeO_2 particle size as observed in the TEM images. And as long as the mesoporous structure can be kept at high uniformity and the CeO_2 particles can be kept small by adjusting the amount of metal loading, the increase of Al can greatly enhance the acetone removal at 150 °C.

3.4. Monometallic versus bimetallic catalysts

Fig. 7 compares the acetone removal efficiency for monometallic Ce–MSPs, Al–MSPs catalysts and bimetallic Ce/Al–MSPs catalyst at temperatures of 150–350 °C. It was observed that the acetone removal was greatly enhanced using bimetallic Ce/Al–MSPs at low temperature range of 150–200 °C as compared to the monometallic Ce–MSPs and Al–MSPs catalysts. The best performance was observed for Ce/Al–MSPs(50/50) which could achieved 80% acetone removal at 150 °C. At temperatures of above 250 °C, the Ce–MSPs and Ce/Al–MSPs appeared to have similar acetone removals, while the acetone removal via Al–MSPs was very poor even up to 350 °C. This indicated that Ce was the active metal for effective acetone removal, especially at relatively higher temperatures. On the other hand, Al played an important role for enhancing the acetone removal at low temperatures. And the co-existence of Ce and Al metal oxides led to a synergetic effect of enhancing the acetone removal.

The synergetic effect was also observed in the literature [27,28] using the Ce/Al–MCM41 as an acylation catalyst. The synergetic effect observed in this study may be explained by literature data [28] which indicated that co-substitution of Ce and Al in MCM-41 during hydrothermal synthesis resulted in a considerable increase in both the density and strength of Lewis acid and Brönsted acid sites as compared with Al–MCM-41 and Ce–MCM-41 samples. If the co-substitution of Ce and Al in MSPs increase the density and strength of the acid sites for acetone oxidation, then it would be undesirable to have excessive increase of Ce loading since it would lead to larger CeO_2 particles present on the surface of MSPs, thus blocking the acid sites and inhibiting acetone removal. This might further explain that Ce/Al–MSPs(25/25) has a lower acetone removal than that of the Ce/Al–MSPs(50/50).

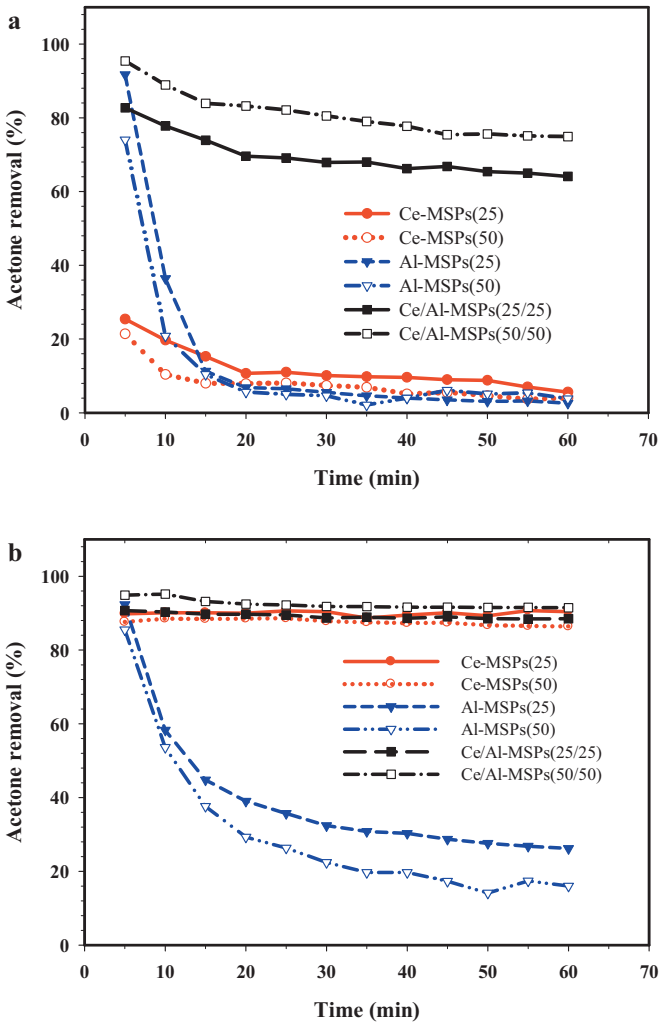

Fig. 8. (a) Short term (60 min) stability tests of acetone removals via Ce–MSPs, Al–MSPs, and Ce/Al–MSPs at operation temperature of 150 °C. (b) Short term (60 min) stability tests of acetone removals via Ce–MSPs, Al–MSPs, and Ce/Al–MSPs at operation temperature of 250 °C.

3.5. Stability Tests

Stability tests were performed first at short operation time of 60 min, the acetone removals were compared between Ce–MSPs, Al–MSPs and Ce/Al–MSPs catalysts and the results are shown in Fig. 8(a) and 8(b), respectively, at two catalytic temperatures of 150 and 250 °C. It was observed that the Al–MSPs exhibited very high acetone removals at both 150 and 250 °C during the initial time. But the acetone removals decreased fast with respect to time, especially during the 150 °C low temperature test results shown in Fig. 8(a). This may indicate that the presence of Al acted as active sites more for adsorption than for catalysis at low temperatures. And the adsorption role of Al–MSPs might decrease while the catalytic role might increase with temperature. It was observed that after the experimental test, the color of Al–MSPs changed from white to black at all temperatures which indicates possible coke formation on the catalytic surfaces [29]. The formation of coke on the Al–MSPs further confirmed that the acetone was adsorbed rather than oxidized on the catalysts.

On the other hand, the Ce–MSPs mainly acted as catalysts. They had low adsorption capacity thus the acetone removals were low

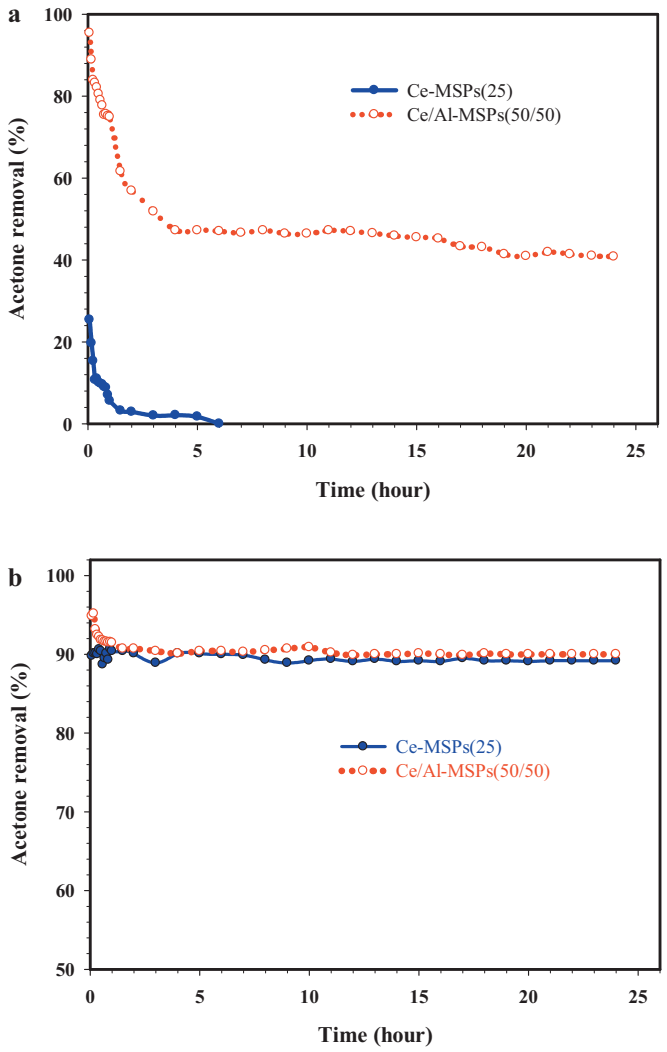

Fig. 9. (a) Long term (24 h) stability tests of acetone removal via Ce–MSPs(25) and Ce/Al–MSPs(50/50) catalysts at operation temperature of 150 °C. (b) Long term (24 h) stability tests of acetone removal via Ce–MSPs(25) and Ce/Al–MSPs(50/50) catalysts at operation temperature of 250 °C.

at temperature of 150 °C. But the catalytic ability of Ce–MSPs was relatively higher than the Al–MSPs, thus acetone removals could remain high and stable at 250 °C during the 60 min operation time. For the bimetallic Ce/Al–MSPs, they had a high stability at 250 °C. On the other hand at low temperature of 150 °C, the acetone removal of Ce/Al–MSPs slightly decreased with respect to time.

To further evaluate the stability of the catalysts, 24 h tests were also performed. The Ce–MSPs(25) had the best acetone removal among all monometallic catalysts, while the Ce/Al–MSPs(50/50) had the best performance among all bimetallic catalysts. Therefore stability tests were performed for these two catalysts at reaction temperatures of 150 °C and 250 °C with the results shown in Fig. 9(a) and (b), respectively. In Fig. 9(a) at the reaction temperature of 150 °C, the acetone removal performance of Ce–MSPs(50/50) decreased significantly during the first 4 h from 95% to 47% and then kept at 40–47% for the rest of time. But the acetone removal of Ce–MSPs(25) was very low from 25% to 0% before the reaction time of 6 h.

On the other hand, in Fig. 9(b) at the reaction temperature of 250 °C, it was observed that the Ce–MSPs(25) could remain high stability on the acetone removal of around 89–91% throughout the 24 h test. But for the Ce/Al–MSPs(50/50), the acetone removal was initially high at over 95% during the first hour test, then it gradually decreased to 91–92% throughout the end of test time, which might be due to that the equilibrium between adsorption and catalysis has been reached. In addition, the color of both catalysts before and after tests remained unchanged. This reveals the high stability of both Ce–MSPs and Ce/Al–MSPs catalysts at 250 °C.

4. Conclusions

Various monometallic and bimetallic–MSPs catalysts were synthesized via one step aerosol EISA method and their catalytic performance on acetone was investigated. The results indicated that bimetallic Ce/Al–MSPs had the best performance among all tested metal catalysts. Catalysts with different Ce/Al molar ratios were then prepared to study the resulting specific surface area of the catalysts and the acetone removals. It revealed that as long as the well mesoporous structure could be maintained with high BET surface areas and smaller CeO_2 particle sizes, the bimetallic Ce/Al–MSPs tended to have a synergetic effect on the acetone removal as compared to the Ce–MSPs or Al–MSPs monometallic catalysts. Both Ce–MSPs(25) and Ce/Al–MSPs(50/50) exhibited good stability during the 24 h tests on acetone removal at 250 °C. In conclusions, the one step aerosol EISA method provides the advantages of easy and time-saving process to produce metal–MSPs catalysts. The Ce/Al–MSPs shall have a high potential for low temperature VOCs oxidation.

Acknowledgement

The authors gratefully acknowledge the financial support from the National Science Council of Taiwan under contract number NSC97-2628-E-009-025-MY2.

References

[1] J.J. Spivey, Industrial and Engineering Chemistry Research 26 (1987) 2165–2180.
[2] B. Skarman, T. Nakayama, D. Grandjean, R.E. Benfield, E. Olsson, K. Niihara, I.R. Wallenberg, Chemistry of Materials 14 (2004) 3686–3699.
[3] Q. Dai, X. Wang, G. Chen, Y. Zheng, G. Lu, Microporous and Mesoporous Materials 100 (2007) 268–275.
[4] Q. Dai, X. Wang, G. Lu, Applied Catalysis B: Environmental 81 (2008) 192–202.
[5] T. Garcia, B. Solsona, S.H. Taylor, Applied Catalysis B: Environmental 66 (2006) 92–99.
[6] C.H. Wang, S.S. Lin, Applied Catalysis A: General 268 (2004) 227–233.
[7] Y. Wu, Y. Zhang, M. Liu, Z. Ma, Catalysis Today 153 (2010) 170–175.
[8] C. Hu, Q. Zhu, Z. Jiang, L. Chen, R. Wu, Chemical Engineering Journal 152 (2009) 583–590.
[9] D. Delimaris, T. Ioannides, Applied Catalysis B: Environmental 89 (2009) 295–302.
[10] G.D. Angel, J.M. Padilla, I. Cuauhtemoc, J. Navarrete, Journal of Molecular Catalysis A: Chemical 281 (2008) 173–178.
[11] T. Mitsui, T. Matsui, R. Kikuchi, K. Eguchi, Topics Catal 52 (2009) 464–469.
[12] J.C.S. Wu, T.Y. Chang, Catalysis Today 44 (1998) 111–118.
[13] Q.H. Xia, K. Hidajat, S. Kawi, Catalysis Today 68 (2001) 255–262.
[14] V.B. Aube, B.L. Monceaux, Applied Catalysis B: Environmental 43 (2003) 175–186.
[15] A.S. Araujo, J.M.F.B. Aquino, M.J.B. Souza, A.O.S. Silva, Journal of Solid State Chemistry 171 (2003) 371–374.
[16] W.B. Li, M. Zhuang, J.X. Wang, Catalysis Today 137 (2008) 340–344.
[17] Z. Mu, J.J. Li, H. Tian, Z.P. Hao, S.Z. Qiao, Materials Research Bulletin 43 (2008) 2599–2606.
[18] W.B. Li, J.X. Wang, H. Gong, Catalysis Today 148 (2009) 81–87.
[19] Y. Lu, H. Fan, A. Stump, T.L. Ward, T. Rieker, C.J. Brinker, Nature 398 (1999) 223–226.
[20] C. Hung, H. Bai, Chemical Engineering Science 63 (2008) 1997–2005.
[21] C. Hung, H. Bai, M. Karthik, Separation and Purification Technology 64 (2009) 265–272.
[22] M.T. Bore, R.F. Marzke, T.L. Ward, A.K. Datye, Journal of Materials Chemistry 15 (2005) 5022–5028.
[23] J.E. Hampsey, S. Arsenault, Q. Hu, Y.F. Lu, Chemistry of Materials 17 (2005) 2475–2480.

[24] M.T. Bore, M.P. Mokhonoana, T.L. Ward, N.J. Coville, A.K. Datye, Microporous and Mesoporous Materials 95 (2006) 118–125.
[25] C.Y. Wang, H. Bai, 13th Asia Pacific Confederation of Chemical Engineering Congress, Taipei, Oct. 5-8, 2010, ID 10088.
[26] S.H. Park, B.Y. Song, T.G. Lee, Journal of Industrial and Engineering Chemistry 14 (2008) 261–264.
[27] M.D. Kadgaonkar, S.C. Laha, R.K. Pandey, P. Kumar, S.P. Mirajkar, R. Kumar, Catalysis Today 97 (2004) 225–231.
[28] P. Kalita, N.M. Gupta, R. Kumar, Journal of Catalysis 245 (2007) 338–347.
[29] Y.C. Lin, H. Bai, C.L. Chang, Journal of the Air and Waste Management Association 55 (2005) 834–840.